**SOIL SCIENCE ANNUAL**
2026, 77(1), 218478

https://doi.org/10.37501/soilsa/218478



# Sustainable nitrogen release and changes in soil properties induced by composite biochar-manure pellets with mineral additives

Tomasz Niedziński[1*], Wojciech Stępień[1], Jan Łabętowicz[1], Wiktoria Wierzchowska[1], Bartłomiej Kowalczuk[1], Katarzyna Szyszkowska[2]

[1] Division of Agricultural and Environmental Chemistry, Institute of Agriculture, Warsaw University of Life Sciences – SGGW, Nowoursynowska Str. 159, 02-776 Warsaw, Poland
[2] Institute of Horticulture – National Research Institute (INHORT), Konstytucji 3 Maja Str. 1/3, 96-100 Skierniewice, Poland

* Corresponding author: Dr Eng. Tomasz Niedziński, tomasz_niedzinski@sggw.edu.pl, ORCID iD: https://orcid.org/0000-0002-4892-5606

Received: 2025-11-24
Accepted: 2026-02-23
Published online: 2026-02-23
Associated editor: Jacek Antonkiewicz

**Keywords:**

Biochar-manure pellets
Nitrogen transformation
Controlled-release fertilizer
Soil buffering capacity
Sustainable nutrient management

**Abstract**

Composite biochar-manure-mineral pellets were evaluated under 100-day incubation conducted under controlled laboratory conditions to elucidate mechanisms controlling nitrogen transformation and soil chemical buffering. Eight formulations combining biochar from various feedstocks, poultry manure, gypsum, lime, and organic substrates were tested on Luvisol soil and designed to represent contrasting pellet chemistries. Soil pH initially increased to 6.7 in lime- and gypsum-enriched variants, then gradually declined, whereas mushroom substrate and fruit-stone biochar maintained near-neutral pH (>6.0) at the end of incubation. Electrical conductivity rose steadily from 102 to 1100–1180 μS $cm^{-1}$ in manure-gypsum treatments, confirming controlled ionic release without salinity stress. Ammonium reached 250 mg N $kg^{-1}$ (G1–G3) before gradually converting to nitrate, which peaked above 200 mg N $kg^{-1}$ by day 100. The rate of Kjeldahl nitrogen change from the granules was moderate, with 62–92% of the initial content remaining at the end of incubation. The results reveal dual-phase kinetics: early nitrate accumulation in soil followed by delayed intra-granular peaks, driven by oxygen diffusion and pH-dependent nitrification. Integration of biochar, gypsum, and lime produced three synergistic buffering effects: temporal (delayed nitrification), chemical (pH stabilization), and hydro-ionic (gradual ECe evolution). These findings establish a basis for designing composite organo-mineral fertilizers that synchronize nitrogen release with soil microbial activity while minimizing acidification and nutrient losses.

## 1. Introduction

Improving nitrogen (N) use efficiency while safeguarding soil health remains a central challenge for sustainable intensification. Biochar highly aromatic, porous carbon produced by pyrolysis has been widely investigated as a soil conditioner capable of modulating pH, increasing cation-exchange capacity (CEC), and altering the soil N cycle through adsorption and microhabitat effects (Abel et al., 2013), (Clough and Condron, 2010), (Glaser et al., 2002), (Jeffery et al., 2011), (Lehmann et al., 2011), (B. Liang et al., 2006). Recent studies show that biochar from organic waste pyrolysis functions as both a carbon sink and a multifunctional soil amendment enhancing nutrient retention and mitigating environmental impacts (Niedziński, et al., 2023). These findings reinforce the potential of waste-derived biochars to serve as a cornerstone of circular nutrient management systems, linking agricultural productivity with environmental protection. Meta-analyses and global syntheses consistently indicate that biochar can enhance plant productivity and nutrient retention, though outcomes are contingent on feedstock, pyrolysis conditions, soil type, and management context (Jeffery et al., 2011), (Lehmann et al., 2011), (Mandal et al., 2015), (Quilliam et al., 2012). Integrating biochar with nutrient-rich manures and mineral dopants into composite pellets therefore offers a purposeful architecture: synchronize N release with crop demand, curb gaseous and leaching losses, and co-deliver improvements to pH, ECe, and structure (Banik et al., 2023), (Malinska et al., 2014), (Mandal et al., 2015), (Wang et al., 2022), (Yurong et al., 2022). Controlled-release concepts using biochar matrices or coatings further delay N dissolution and raise apparent recovery in pots, greenhouses, and fields (Banik et al., 2023), (Niedziński et al., 2021), (Sriraj and Butnan, 2024). At the mechanism scale, biochar surfaces sorb $NH_4^+$ and organic N, buffer pH, and shape redox microgradients that steer nitrification-denitrification (Abel et al., 2013), (Clough and Condron, 2010), (Glaser et al., 2002), (Biqing Liang et al., 2006), (Wang et al., 2022). During manure co-composting and soil application, biochar consistently suppresses $NH_3$ and $N_2O$ losses and fosters humified N forms (Alomari et al., 2024), (Fauzan et al., 2025), (Goulding, 2016), (Malinska et al., 2014), (Mandal et al., 2015). Pelleting organo-mineral blends adds granule integrity and engineered release profiles (Fávero et al., 2006). Among dopants, gypsum ($CaSO_4 \cdot 2H_2O$) supplies $Ca^{2+}/SO_4^{2-}$, enhances aggregation, and repeatedly reduces particulate and dissolved P losses at field-catchment scales (Ekholm et al., 2024), (Ekholm et al., 2012), (Sumner et al., 1986); lime ($CaCO_3$) elevates pH, alleviates Al toxicity, and sustains nitrifiers, though $NH_3$ and $N_2O$ responses are context-specific and best buffered by sorptive carbon scaffolds (Atkinson et al., 2010), (Rebecca, 2023), (Skuta et al., 2025), (Sun et al., 2024). Feedstock composition further tunes these functions: bran contributes labile C-N that transiently immobilizes N and tempers early $NH_3$ before giving way to nitrification (Hou et al., 2018), (Oarga et al., 2019), (Oarga et al., 2016); cone-derived biochar raises CEC and sorbs mineral N, slowing release and stabilizing pH (Igalavithana et al., 2017); fruit-stone biochar improves physical structure while compost or compost-biochar blends elevate chemical-biological fertility (Calvano and Tamborrino, 2022), (Fornes et al., 2024). Critically, placement depth governs how these traits manifest in planta: deep placement of slow-release granules (20 cm) in potato re-allocated biomass, increased N and P uptake, and stimulated root system development, which is evidence that spatial targeting can synchronize supply with root foraging and water regimes (Niedziński, Rutkowska, et al., 2023). Incubation and field evidence underscores the design logic. Mineral N granules can dissolve rapidly in calcareous soils (>70–98% within days), spiking ECe and perturbing pH, whereas organic or biochar-based pellets pace release and retain N in the matrix (Niedziński et al., 2021). Recent work shows biochar-manure systems sustain fertility, tune $NH_4^+ \leftrightarrow NO_3^-$ speciation, raise CEC, and temper salinity in sandy or saline-alkaline settings (Fauzan et al., 2025), (Sriraj and Butnan, 2024); long-term datasets indicate that blending organic inputs with minerals preserves soil N stocks and micronutrient status relative to purely mineral regimes (Olifir et al., 2024). Across environments, biochar-based organics frequently improve N-use efficiency and crop performance, arguing for composite granules tailored to soil constraints, root distribution, and demand curves (Alomari et al., 2024), (Niedziński, et al., 2023). In Poland, the agricultural use and marketing of biochar-based fertilising products is shaped by both EU and national regulations. Products that meet the requirements for EU fertilising products may be placed on the market with CE marking under Regulation (EU) (2019/1009) which also recognises pyrolysis and gasification materials as a component material category for EU fertilising products.

Despite extensive research on biochar and manure-based amendments, the data are still limited on composite biochar-manure granules combined with mineral additives and their time-dependent effects on the partitioning of mineral N between $NH_4^+$-N and $NO_3^-$-N, and concurrent shifts in key soil-solution proxies such as pH and electrical conductivity (ECe) under controlled incubation conditions (without plant uptake or leaching). In particular, the extent to which mineral additives can change nitrification-driven acidification and ionic strength during N release remains insufficiently quantified for very sandy and low-buffering topsoil. Therefore, the aim of this study was to quantify, over a 100-day incubation, the effects of composite biochar-manure pellets with different mineral additives on the dynamics of $NH_4^+$-N and $NO_3^-$-N, and on pH and ECe, under constant temperature and moisture. We evaluate composite biochar-manure pellets with and without gypsum or lime under soil incubation conditions, quantifying changes in pH, electrical conductivity, mineral nitrogen ($NH_4^+$, $NO_3^-$), and Kjeldahl nitrogen over time. We hypothesize that (H1) biochar and manure composites slow down nitrogen release and increase its retention; (H2) gypsum mitigates ionic strength and stabilizes $NH_4^+$, while limiting $NO_3^-$ accumulation, and (H3) lime raises pH to control nitrification, and biochar buffers the risk of volatilization. By combining the chemistry of the preparations with real-time measurements and conclusions based on analysis of variance (ANOVA), we aim to determine how the composition of the granules and their distribution affect the sustainable supply of nitrogen and changes in soil properties.

## 2. Materials and methods

### 2.1. Study of organic granulates

This research was carried out in laboratory conditions in the Experimental Station in Skierniewice, belonging to Warsaw University of Life Sciences. Eight granulated composted organic materials with mineral additives were incubated in soil sampled from arable field from Skierniewice. The incubation was established on Luvic Stagnosol derived from sandy loam soil (IUSS Working Group WRB, 2015). The granulated organo-mineral pellets were prepared in an experimental station on a pilot installation for pellet production in Skierniewice, Poland. The fertilizer granules consisted of various organic materials containing organic biomass: biochar made of cone, bark, bran, ground fruit stone, enriched with poultry manure, mashroom substrate and mineral components. Biochar from bran was produced via multi-stage pyrolysis, with vegetable oils as the primary products, and the remaining biochar was a waste product of this process, used in research on its usefulness as a soil improver with other mineral additives. Eight different fertilizer mixtures were produced by pelletizing, consisting of the following components mixed in volume proportions v/v (Table 1, Fig. 1). The proportions of ingredients in the granule formulations were selected a priori to obtain mechanically stable granules suitable for handling and incubation, while ensuring (i) a measurable source of nitrogen (manure fraction) during 100 days of incubation, (ii) a sufficient biochar fraction to influence the chemical composition of the soil solution, and (iii) sufficient mineral additives to examine buffering/ionic effects without dominating the formulation. The chemical parameters of the granules were measured using the same methods as for soil: Kjeldahl nitrogen, mineral nitrogen using CFA, with extraction in distilled water at a mass/volume ratio of 1:5 (m/v).

The scope of this study regarding biochar composition is limited; it focuses on the overall (net) response of the soil to composite granules of biochar and manure with mineral addi-

**Table 1**
Granule components and volume proportions of granule mixtures used for incubation in soil

| Granulate | Components | Volumetric Ratio |
|---|---|---|
| G1 | Cone biochar + Poultry manure + Gypsum | 2:2:1 |
| G2 | Bark biochar + Poultry manure + Gypsum | 2:2:1 |
| G3 | Bark biochar + Poultry manure + Gypsum + Lime | 2:2:0.5:0.2 |
| G4 | Fruit stone biochar + Poultry manure + Mushroom substrate | 2:1:2 |
| G5 | Bran biochar + Poultry manure + Mushroom substrate | 2:1:2 |
| G6 | Fruit stone biochar + Poultry manure + Mushroom substrate | 2:1:2 |
| G7 | Bran biochar + Poultry manure + Gypsum | 2:2:1 |
| G8 | Bran biochar + Poultry manure + Mushroom substrate | 2:1:2 |

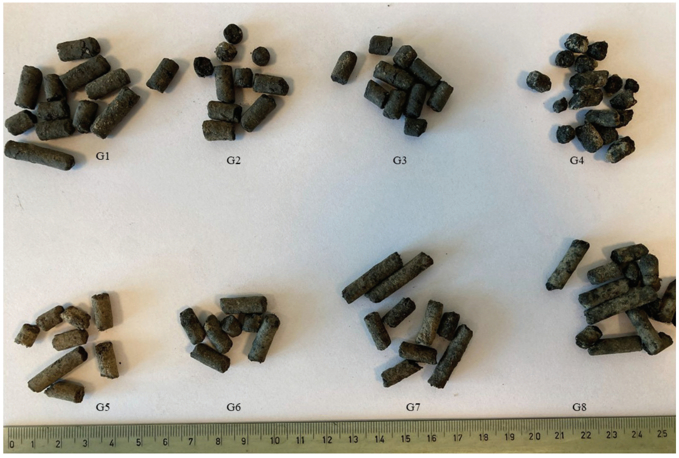


**Fig. 1.** Granules used in soil incubation experiment, G1–G4 upper line from left to right, G5–G8 bottom line from left to right (photo: T. Niedziński)

tives. Changes in $NH_4^+$-N, $NO_3^-$-N, pH, and ECe were quantified during a 100-day incubation period to describe the integrated fertilizing and physicochemical effects of these composites. Detailed chemical characterization of individual biochar types (e.g., organic carbon, total nitrogen, phosphorus, potassium, pH, ash, and trace contaminants) was beyond the scope of this article and will be presented separately; therefore, mechanistic attribution of properties to a given biochar should be interpreted with caution.

## 2.2. Study soil

The soil was collected from the 0–20 cm layer of cultivated soil at the Experimental Station of Warsaw University of Life Sciences in Skierniewice, central Poland, which is under the influence of a temperate, warm, transitional climate combining characteristics of a Maritime and Continental climate. The average particle-size distribution of the incubated soil was: sand 89%, silt 6%, and clay 5%, indicating a very sandy texture (loamy sand). Soil pH was measured in a 1 M KCl solution (1:2.5) using a potentiometric method (ISO 10390: 2005) with a pH meter (Schott, Mainz, Germany, type GC 842). Soil electric conductivity was measured in a distilled water (1:5), using a conductometer (Mettler Toledo, Germany). Ammonium and nitrate nitrogen were measured in a 1% $K_2SO_4$ solution in a 1:10 ratio (Siewruk and Szulc, 2023), using continuous flow analysis (CFA-Continuous Flow Analysis) using Skalar San apparatus (The Netherlands) with a cadmium column. The Kjeldahl nitrogen in soil (ISO 11261:1995) was measured using VELP Scientifica distillation apparatus. Field capacity (FC) was determined by saturating a cylinder filled with soil and allowing it to drain freely by gravity until downward water movement became negligible. Throughout the incubation period, 60% of the FC of the soil was maintained. The accuracy and reliability of the analytical results were ensured through regular calibration of the instruments using laboratory-prepared standard solutions and routine analysis of control samples. Analytical precision was verified by performing replicate measurements, and results were subject to internal quality control procedures.

## 2.3. Experimental design and statistical analysis

Each granule was placed and covered with soil. Proportions of 1 to 50 (10 g of fertilizer and 500 g of soil) were arranged in rectangular boxes measuring 25 cm × 15 cm × 4 cm. The experiment was conducted in a randomized system as follows: 8 granules × 5 incubation periods × 3 replicates = 120 treatments. After incubation, the granules and soil were separated and dried at room temperature. The crushed and ground samples of the separated granules and soil were analysed chemically. Sampling took place after 10, 20, 40, 70, and 100 days. Throughout the incubation period, 60% of the maximum water retention capacity was maintained. Adequate soil moisture was maintained by regularly weighing the samples; when soil moisture decreased, the water deficit was replenished. Distilled water was used for irrigation. Statistical differences were assessed using analysis of variance (ANOVA), applying Tukey's procedure for homogeneous groups. Statistical analysis was performer using STATISTICA 13.1 software. The significance level of the analysis was α = 0.05.

## 3. Results

### 3.1. Soil pH

The soil pH showed a gradual but distinct transformation during the 100-day incubation, with the magnitude and direction of change strongly dependent on the granulate composition. At the beginning (day 0), the pH across all treatments was close to 6.0, confirming homogeneous initial conditions (Fig. 2). Over time, however, the patterns of acidification diverged, reflecting the different physicochemical properties of the granulates. Separate one-way ANOVA analyses for each treatment, comparing pH values against the control at each incubation stage, revealed statistically significant differences ($p < 0.05$), further detailed by Tukey's test. During the first 10–20 days, most variants remained close to the control, indicating that initial decomposition processes had not yet markedly altered soil reaction. Nonetheless, G2 (bark biochar + poultry manure + gypsum) and G3 (bark biochar + poultry manure + gypsum + lime) exhibited slightly higher pH, suggesting early alkalinization due to the presence of bark-derived ash and, in the case of G3, additional calcium from lime. The lime component in G3 likely enhanced the soil's buffering capacity, delaying acid formation. In contrast, G5, G7, and G8 rich in bran, poultry manure, and mushroom substrate showed subtle pH fluctuations around neutrality, reflecting the onset of organic acid production during the mineralization of easily degradable organic matter. By day 40, statistically significant differentiation between treatments became evident. G3 reached the highest pH (6.8, distinctly exceeding the control (5.9) and the more acidified formulations, such as G2 and G8 (pH 5.6–5.9). The pronounced liming effect of G3 underscores the synergistic role of bark, lime, and gypsum in maintaining near-neutral soil conditions through enhanced cation exchange and carbonate buffering. Granulates with mushroom substrate (G5 and G6) also maintained relatively stable pH (6.2–6.3), likely due to the slow decomposition of lignocellulosic residues and the high sorptive capacity of the fungal matrix, which helps retain exchangeable base cations. From day 70 onward, the pH decline became more pronounced.

and statistically significant across all variants. Acidification was strongest in G1-G3, where pH dropped below 5.5. The rapid pH decrease in these treatments can be attributed to the combined effect of poultry manure mineralization and the limited buffering of cone and bark biochar once their surface alkalinity was exhausted. Conversely, G5 and G6 preserved higher pH (> 6.0), reflecting the stabilizing influence of mushroom substrate and fruit-stone biochar, both of which decompose slowly and release fewer organic acids over time. By day 100, the cumulative effect of incubation time and granulate composition became fully apparent. The control soil reached pH 5.5, which could have been the result of net mineralization of organic nitrogen followed by nitrification of the released $NH_4^+$, causing soil acidification, while the most acidified treatments (G1-G3 and G8) decreased to 5.1–5.4, significantly lower than at earlier stages. In contrast, G5 (5.9) and G7 (5.6) maintained higher pH, remaining statistically different from the control ($p < 0.05$). These results indicate that the inclusion of mushroom substrate and bran components provided lasting pH stabilization, likely through gradual nutrient release and increased base cation retention. The statistical and compositional analyses reveal that soil pH evolution was governed by both the duration of incubation and the specificity of chemical composition of each granulate. Mixtures enriched with alkaline agents (lime, gypsum) or slowly decomposing organic matrices (mushroom substrate, fruit-stone biochar) effectively moderated acidification, while those dominated by bark or cone biochar combined with poultry manure enhanced proton accumulation and pH decline. The data indicate that the balance between mineral buffering components and organic degradability is critical for maintaining soil chemical stability during incubation with organic amendments.

### 3.2. Soil electrical conductivity

Soil electrical conductivity (ECe) increased progressively during the 100-day incubation, with clear effects of granulate composition. Initially, conditions were uniform (102 µS cm$^{-1}$). As incubation progressed, results confirmed significant differences ($p < 0.05$), reflecting the distinct ion-release patterns of each formulation (Fig. 3). Even after 10 days, ECe rose sharply in all amended soils compared to the control. The highest increases

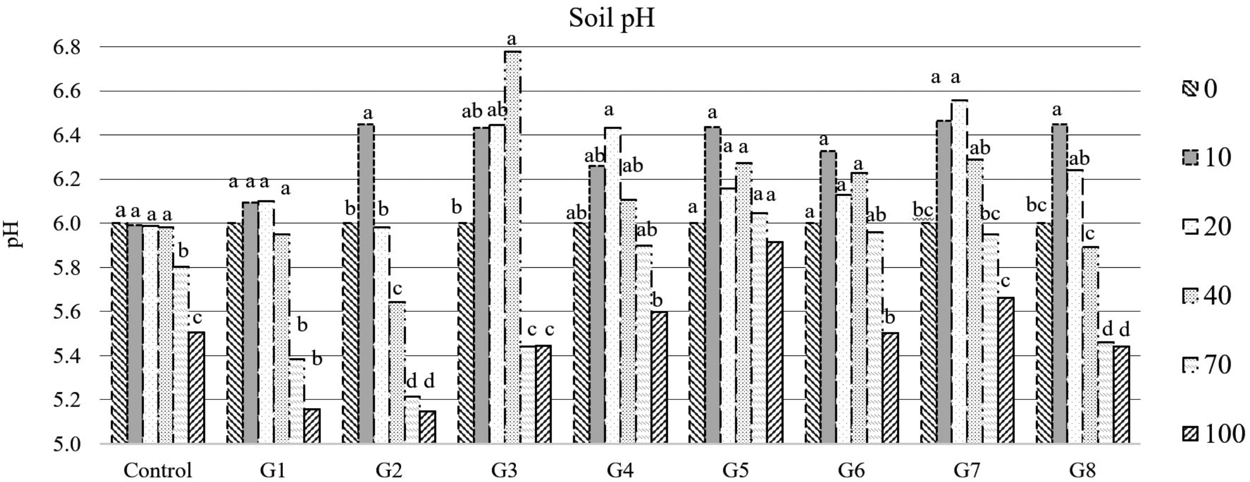


**Fig. 2.** Effect of incubation time of granules on soil pH; *values are mean, the letters indicate a significant difference from one another based on Tukey's test at $p < 0.05$

occurred in G1 (879 μS cm⁻¹) and G3 (626 μS cm⁻¹), indicating rapid dissolution of soluble salts from poultry manure, lime, and gypsum. Granulates with gypsum or lime (G2, G4, G6) also showed elevated ECe (480–540 μS cm⁻¹), while those containing mushroom substrate or bran (G5, G6) displayed slower ion release (350 μS cm⁻¹).

As incubation progressed (20–70 days), ECe continued to rise significantly ($p < 0.05$), reaching 1183 μS cm⁻¹ in G1 and 1102 μS cm⁻¹ in G7. These high values reflected intensified mineralization of manure-derived nitrogen and sulphur compounds. Treatments containing mushroom substrate or fruit-stone biochar (G5, G6, G8) remained more stable (600–860 μS cm⁻¹), suggesting gradual nutrient solubilization and better ionic buffering. The control remained far lower (below 219 μS cm⁻¹), confirming that the effect resulted from the amendments. The test showed a significant increase in electrical conductivity, reflecting the fact that the accumulation of soluble ions formed during mineralization/nitrification in a system without uptake by plants or leaching resulted in significantly higher electrical conductivity (ECe). By day 100, ECe remained several times higher than the control (378 μS cm⁻¹), with the highest final values in G1 (1120 μS cm⁻¹), G7 (1151 μS cm⁻¹), and G8 (938 μS cm⁻¹). Intermediate levels occurred in G3 and G5 (740–780 μS cm⁻¹), while G6 remained lowest among amended soils. Altogether, the data indicate that both incubation time and composition determined ECe evolution. Granulates rich in poultry manure and gypsum (G1, G7) caused rapid and sustained salinity increases, whereas those with mushroom substrate or biochar (G5, G6, G8) released ions more gradually, maintaining a more balanced electrochemical environment in the soil.

### 3.3. Ammonium nitrogen in soil

Soil ammonium dynamics during incubation were strongly shaped by the presence and composition of the granulated composts, with pronounced but transient accumulation in several treatments (Fig. 4). At day 0, all soils showed comparable $NH_4^+$ levels (44.9 mg $N\text{-}NH_4$ kg⁻¹), confirming uniform starting conditions. Subsequent measurements revealed rapid increases in amended variants.

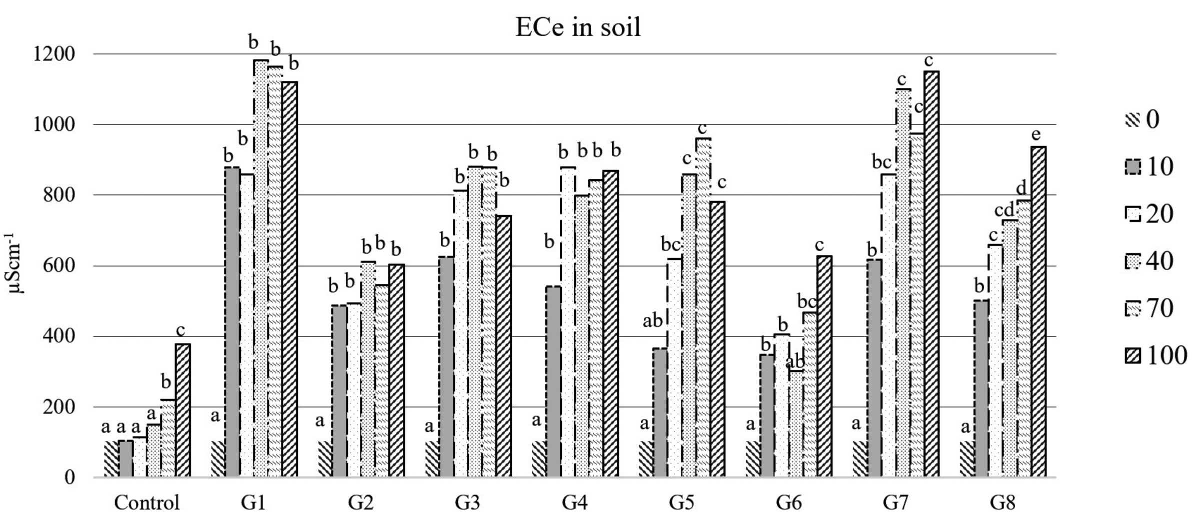


**Fig. 3.** Effect of incubation time of granules on electric conductivity in soil (μS cm⁻¹); *values are mean, the letters indicate a significant difference from one another based on Tukey's test at $p < 0.05$

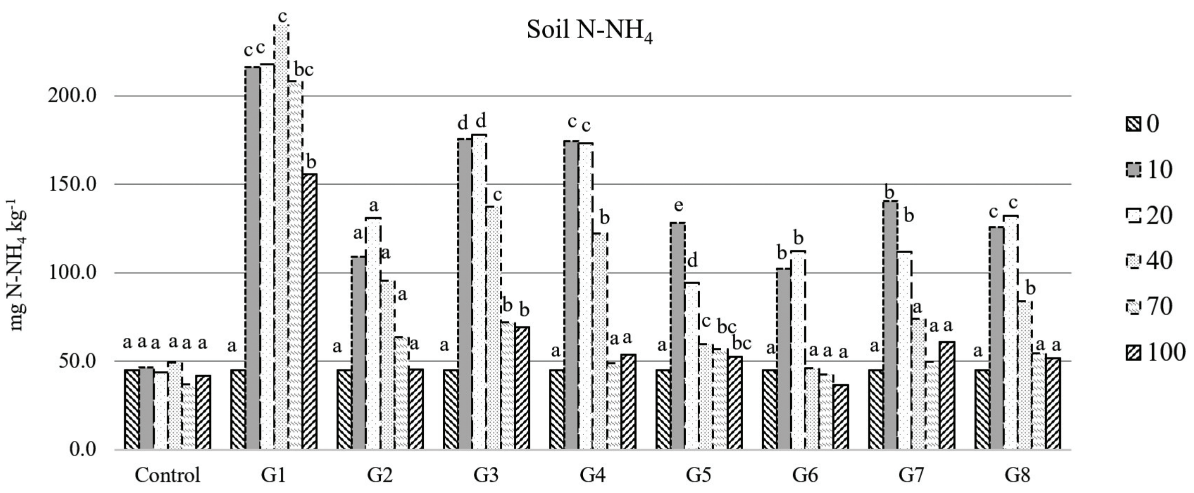


**Fig. 4.** Effect of incubation time of granules on ammonium nitrogen content in soil (mg $N\text{-}NH_4$ kg⁻¹); *values are mean, the letters indicate a significant difference from one another based on Tukey's test at $p < 0.05$

The most distinct response occurred in granulates with high poultry manure input and mineral carriers. G1 (cone biochar + manure + gypsum) and G3 (bark biochar + manure + gypsum + lime) generated sharp and sustained $NH_4^+$ surges, reaching 216–218 mg kg$^{-1}$ already at day 10–20 and peaking at 252 mg kg$^{-1}$ (G1) at day 40, consistently and significantly exceeding the control. Elevated concentrations were also recorded for G4 (fruit stone biochar + manure + mushroom substrate) and G8 (bran biochar + manure + mushroom substrate), particularly up to day 20, indicating efficient N mineralization coupled with slower organic matrices. In contrast, G2 (bark biochar + manure + gypsum) and especially G5 (bran + manure + mushroom substrate) and G6 (fruit stone biochar + manure + mushroom substrate) showed more moderate increases and a faster decline toward control levels, pointing to tighter N retention or accelerated nitrification. From day 40 onward, all treatments exhibited a gradual decrease in $NH_4^+$, and by day 100 only G1 and, to a lesser extent, G3 maintained clearly higher concentrations (156 and 69 mg kg$^{-1}$) than the unamended soil (42 mg kg$^{-1}$), while the remaining granulates converged with the control. Overall, the data indicate that the granules differed mainly in the intensity and persistence of ammonium release: manure- and gypsum-rich formulations, particularly G1 and G3, promoted strong and prolonged $NH_4^+$ accumulation, whereas mixtures containing mushroom substrate and specific biochars moderated this response, favouring a shorter and less pronounced ammonium peak.

### 3.4. Nitrate nitrogen in soil

Soil nitrate concentrations responded strongly to both incubation time and the nature of the granulated composts. At day 0, all treatments were uniform (8.9 mg N-$NO_3$ kg$^{-1}$), indicating identical initial conditions (Fig. 5). Thereafter, nitrate remained low and comparable to the control during the first 10 days, showing that nitrification was still limited at this stage. A clear divergence appeared from day 20 onward. Granulates combining poultry manure with mineral or structurally stable carriers (G2, G3, G4, G6, G8) generated a rapid rise in $NO_3^-$, with values of 43–46 mg kg$^{-1}$ in G2-G4 and over 69 mg kg$^{-1}$ in G8, significantly surpassing the control (9.7 mg kg$^{-1}$). By day 40, G1 (cone biochar + manure + gypsum) reached about 117 mg kg$^{-1}$ and G8 over 91 mg kg$^{-1}$, while the control remained below 14 mg kg$^{-1}$, confirming efficient conversion of organic N to nitrate in manure-based granules supported by biochar, gypsum or mushroom substrate. From 40 to 100 days, nitrate accumulation intensified rather than declined, demonstrating sustained nitrification.

At 70 days, all amended soils showed markedly higher $NO_3^-$ contents (typically 100–163 mg kg$^{-1}$) relative to the control (23 mg kg$^{-1}$), with particularly strong responses in G1, G2, G3 and G4. By the end of incubation, nitrate levels peaked: G1, G4 and G3 exceeded 199–207 mg kg$^{-1}$, and all other granulates, including G8 (172 mg kg$^{-1}$), remained far above the control (74.6 mg kg$^{-1}$), with statistically distinct groupings among treatments. It was also shown that the incubation conditions themselves favoured basic microbiological processes, including the mineralization of native organic nitrogen and subsequent nitrification, increasing the concentration of $NO_3^-$ in the soil. Taken together, the results indicate that all granulated formulations substantially enhanced nitrate availability over time, with the most pronounced and persistent increases in granules combining poultry manure with gypsum, lime or mushroom substrate (G1-G4, G8). These compositions evidently provided both ample ammonium substrate and favourable conditions for nitrification, leading to a strong and prolonged enrichment of soil $NO_3^-$.

### 3.5. Ammonium nitrogent in granules

Ammonium nitrogen content declined consistently across all composite biochar-manure pellets during the 100-day incubation period, with the rate and magnitude of reduction varying among formulations (Table 2). At the onset (day 0), the highest $NH_4^+$ levels were found in G1 (744.2 mg N-$NH_4$ kg$^{-1}$) and G7 (399.1 mg kg$^{-1}$), while G2 (238.6 mg kg$^{-1}$) and G6 (297.3 mg kg$^{-1}$) contained comparatively less. Over time, all treatments experienced a gradual decrease, reflecting progressive mineralization and nitrification processes. By day 40, G1 retained the highest ammonium concentration (566.5 mg kg$^{-1}$; 76% of initial), followed by G7 and G8, whereas G4-G6 dropped below 30–35% of their initial values.

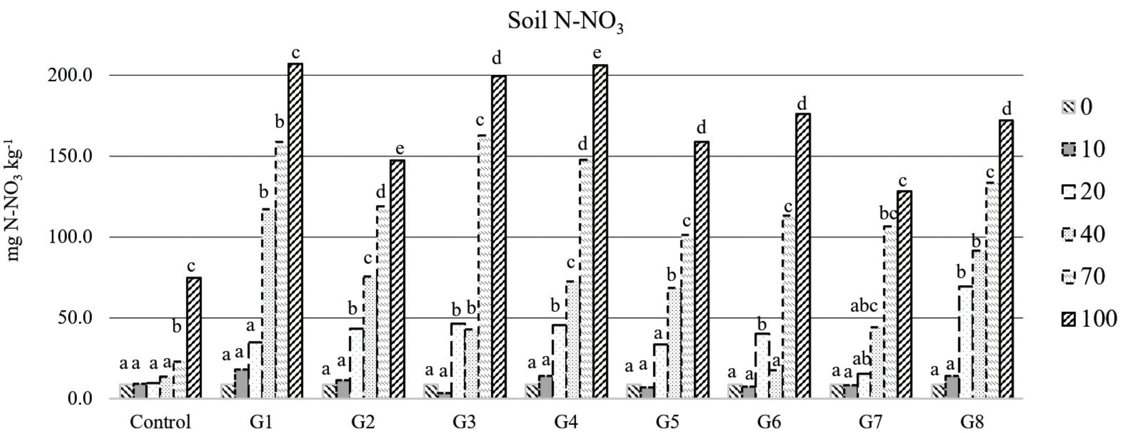


**Fig. 5.** Effect of incubation time of granules on nitrate nitrogen content in soil (mg N-$NO_3$ kg$^{-1}$); *values are mean, the letters indicate a significant difference from one another based on Tukey's test at $p < 0.05$

**Table 2**
Effect of incubation time on ammonium nitrogen content (mg N-$NH_4$ $kg^{-1}$) in granulated organic compounds

| Days | G1 | Relative % | G2 | Relative % | G3 | Relative % | G4 | Relative % | G5 | Relative % | G6 | Relative % | G7 | Relative % | G8 | Relative % |
|---|---|---|---|---|---|---|---|---|---|---|---|---|---|---|---|---|
| 0 | 744a | 100 | 239a | 100 | 331a | 100 | 357a | 100 | 381a | 100 | 297a | 100 | 399a | 100 | 349a | 100 |
| 10 | 677ab | 91 | 217ab | 91 | 301ab | 91 | 324a | 91 | 347a | 91 | 270a | 91 | 363a | 91 | 317a | 91 |
| 20 | 608abc | 82 | 174b | 73 | 266abc | 80 | 319a | 90 | 233b | 61 | 248a | 83 | 331.4a | 83 | 287ab | 82 |
| 40 | 566bc | 76 | 102c | 43 | 119bc | 36 | 99b | 28 | 78c | 20 | 103b | 35 | 223b | 56 | 223bc | 64 |
| 70 | 507c | 68 | 87c | 37 | 46c | 14 | 55b | 15 | 54c | 14 | 64b | 22 | 45c | 11 | 143cd | 41 |
| 100 | 330d | 44 | 44c | 18 | 43d | 13 | 61b | 17 | 51c | 13 | 78b | 26 | 72c | 18 | 86d | 25 |

*values are means, the letters indicate a significant difference from one another based on Tukey's test at $p < 0.05$

The most pronounced reduction occurred in G3 and G5, where ammonium content fell to around 36% and 20% of the baseline, respectively, suggesting a faster conversion of $NH_4^+$ to nitrate in these mixtures. At the end of incubation (day 100), all granulates showed substantial depletion, with residual $NH_4^+$ ranging from 13% (G3, G5) to 44% (G1) of the initial level. The relatively higher retention in G1 indicates a slower mineralization rate and a more prolonged release pattern, likely related to the buffering role of cone biochar and gypsum. In summary, incubation time had a decisive impact on ammonium nitrogen decline, but the persistence of $NH_4^+$ differed markedly with granulate composition. G1 maintained the highest ammonium content throughout, while G3 and G5 exhibited the most rapid transformation, highlighting compositional control over nitrogen stabilization and turnover in organic granulated amendments.

### 3.6. Nitrate nitrogent in granules

Nitrate nitrogen in the granulated materials displayed a clear shift from early depletion to pronounced late-stage accumulation, strongly modulated by granulate composition and incubation time (Table 3). At day 0, nitrate contents were relatively low and formulation-specific (from 3.40 mg N-$NO_3$ $kg^{-1}$ in G1 to 81.2 mg $kg^{-1}$ in G2 and 77.6 mg $kg^{-1}$ in G6). During the first 10–40 days, all granules showed a marked decline to only a few percent of their initial nitrate, with G5, G6, G3 and G8 approaching near-complete depletion, indicating rapid consumption or transformation of the initial $NO_3^-$ pool.

After 70 days, this pattern reversed, and nitrate accumulated sharply within the granules. Very strong increases were recorded in G1, G3 and G8, where contents rose to 134–275 mg $kg^{-1}$ at day 70 and further to about 258–299 mg $kg^{-1}$ at day 100, representing several-fold to several-tens-fold increases relative to their starting levels. By the end of incubation, all treatments exhibited substantially elevated nitrate (≥170 mg $kg^{-1}$), with consistently high values in G1, G2, G3, G4, G6 and G8, demonstrating effective conversion of organically bound N into nitrate within the granulated matrices.

### 3.7. Kjeldahl nitrogen in granules

Kjeldahl nitrogen in the granules declined gradually during incubation, but the extent of this loss varied with formulation. At day 0, G8 and G1 contained the highest N levels (36.03 and 26.40 g N $kg^{-1}$), whereas G2-G5 showed lower initial contents

**Table 3**
Effect of incubation time on nitrate nitrogen content (mg N-$NO_3$ $kg^{-1}$) in granulated organic compounds

| Days | G1 | Relative % | G2 | Relative % | G3 | Relative % | G4 | Relative % | G5 | Relative % | G6 | Relative % | G7 | Relative % | G8 | Relative % |
|---|---|---|---|---|---|---|---|---|---|---|---|---|---|---|---|---|
| 0 | 3.4c | 100 | 81.2b | 100 | 8.4c | 100 | 34.1b | 100 | 28.5c | 100 | 77.6b | 100 | 34.6c | 100 | 16.1b | 100 |
| 10 | 3.1c | 91 | 73.8bc | 91 | 7.7c | 91 | 30.9b | 91 | 25.9c | 91 | 70.5b | 91 | 31.4cd | 91 | 14.6b | 91 |
| 20 | 0.55c | 16 | 42.4cd | 52 | 1.1c | 13 | 4.3b | 13 | 1.06d | 4 | 0.40c | 0 | 5.8de | 17 | 0.77b | 5 |
| 40 | 1.5c | 46 | 26.4d | 33 | 0.89c | 10 | 0.37b | 1 | 1.75d | 6 | 0.27c | 0 | 1.4e | 4 | 2.78b | 17 |
| 70 | 134.5b | 3957 | 20.7d | 26 | 179.2b | 2116 | 6.4b | 19 | 83.0b | 291 | 114.3b | 147 | 83.9b | 243 | 275.3a | 1710 |
| 100 | 298.3a | 8778 | 231.2a | 285 | 258.0a | 3046 | 241.4a | 709 | 170.1a | 597 | 255.3a | 329 | 222.7a | 644 | 266.5a | 1656 |

*values are means, the letters indicate a significant difference from one another based on Tukey's test at $p < 0.05$

**Table 4**
Effect of incubation time on Kjeldahl nitrogen content (g N $kg^{-1}$) in granulated organic-mineral composites

| Days | G1 | Relative % | G2 | Relative % | G3 | Relative % | G4 | Relative % | G5 | Relative % | G6 | Relative % | G7 | Relative % | G8 | Relative % |
|---|---|---|---|---|---|---|---|---|---|---|---|---|---|---|---|---|
| 0 | 26.4a* | 100 | 11.2a | 100 | 11.7a | 100 | 15.7a | 100 | 19.1a | 100 | 25.5a | 100 | 21.7ab | 100 | 36.0a | 100 |
| 10 | 25.9a | 98 | 10.8a | 97 | 11.1a | 94 | 15.4a | 98 | 18.7a | 98 | 24.1a | 95 | 22.1a | 102 | 35.8a | 100 |
| 20 | 24.0ab | 91 | 10.5a | 95 | 9.3ab | 80 | 13.5ab | 86 | 14.6b | 77 | 21.5b | 84 | 20.4ab | 94 | 35.4ab | 98 |
| 40 | 22.7b | 86 | 9.3ab | 83 | 8.1b | 69 | 11.9bc | 76 | 11.9c | 62 | 19.8bc | 78 | 20.8ab | 96 | 33.9bc | 94 |
| 70 | 19.5c | 74 | 7.7b | 69 | 7.2c | 61 | 10.4c | 67 | 10.4d | 55 | 20.2bc | 79 | 19.9ab | 92 | 32.9c | 91 |
| 100 | 19.5c | 74 | 9.1ab | 81 | 7.2c | 62 | 10.4c | 66 | 11.8cd | 62 | 19.2c | 75 | 19.4b | 89 | 33.1c | 92 |

*values are means, the letters indicate a significant difference from one another based on Tukey's test at $p < 0.05$

(11.17–19.13 g N $kg^{-1}$) (Table 4). Over 100 days, all granulates exhibited statistically supported reductions (Tukey, $p < 0.05$ for key contrasts), yet the decrease was only partial, indicating effective N retention within most matrices.

The most pronounced preservation was observed in G8 and G7, which still maintained about 92% and 89% of their initial Kjeldahl N at day 100 (33.16 and 19.39 g N $kg^{-1}$, respectively), and in G2 and G6 (75–81% of initial). In contrast, G3, G4 and G5 showed stronger relative depletion, stabilizing at around 61–66% of their starting values. G1, despite a noticeable decline to 74% of its initial content, remained among the N-richest materials at the end of the incubation. Taken together, the data indicate that incubation did not lead to drastic Kjeldahl N exhaustion within the granules; instead, several formulations particularly G7 and G8 acted as stable N reservoirs, while others (G3–G5) released organic N more readily, suggesting compositional control over the balance between N conservation and mobilization.

## 4. Discussion

Incubation data indicate that granules consisting of biochar and manure with added minerals cause coupled changes in soil chemistry and nitrogen cycling: initially buffered pH increase in the zone of contact between granules and soil, gradual increase in electrical conductivity (ECe) associated with sustained ion release. A similar initial trend of stable pH was obtained after one week of incubation of manure and manured biochar, with a tendency for pH to increase from 6.6 to 6.7–6.8 (Firnass et al., 2023), (Lebrun et al., 2023), (Yang et al., 2025), (Zhang et al., 2024). According to Chintalaa et al. (2013), corn stover and switchgrass biochar, and lime at doses ranging from 0 to 156 Mg $ha^{-1}$, affected soil pH. The increase in soil pH was most pronounced during the first 15 days of incubation in clay loam soil with an initial pH of 4.7, reaching a maximum with corn stover biochar (raising pH by 0.73–1.36 units) and liming. The type of biochar and the addition of mineral-based materials, such as lime, determine the intensity of its impact on soil properties (e.g., G3 granules) (Skuta et al., 2025).

The soil ECe values were steeper in granules containing gypsum or lime, which is consistent with the mechanism of prolonged release of $Ca^{2+}$, $SO_4^{2-}$, and $HCO_3^-/CO_3^{2-}$ from mineral carriers and salts derived from manure, increasing the ionic strength of the solution (Ekholm et al., 2024). Therefore, the gradual increase in ECe observed in this study does not necessarily indicate a risk of agronomic salinity, provided it is regulated by calcium-rich electrolytes. Similar two- to five-fold ECe increases have been reported after adding biochar to acidic or sandy soils, often reaching **0.3–0.4 dS $m^{-1}$ (300–400 µS $cm^{-1}$)** without yield penalties (Pandian et al., 2024). The slower ECe build-up in pellets with mushroom substrate and fruit-stone biochar suggests that more recalcitrant organic matrices and different pore structures modulate ion diffusion, echoing observations that biochar-manure blends can increase nutrient availability while avoiding excessive salinity (Lebrun et al., 2023), (Gao et al., 2022). The ECe of soil is influenced by the type of biochar, mineral additives, and dosage. Treating soil with biochar or lime with an ECe of 92 **µS $cm^{-1}$** (similar to the soil used in the experiment) increases the value depending on the type and dosage of the soil improver. The use of doses of 52–156 Mg $ha^{-1}$ resulted in an increase in soil ECe to 113–240, 110–146, and 706–713 uS $cm^{-1}$ for biochar from corn stover, switchgrass, and lime, respectively (Chintalaa et al., 2013). It should be noted that the incubation soil in our study was very sandy (loamy sand; 89% sand), whereas Chintala et al. (2013) used a clay loam soil. Because soil texture strongly affects buffering capacity and ion retention, the cited study is used here primarily to illustrate the general pH response to biochar/lime. Nitrogen distribution confirms the path of retention followed by release. The total Kjeldahl nitrogen content in the pellets decreased slowly, with carbon-rich pellets with high CEC showing the smallest changes – in line with $NH_4^+$ sorption on oxidized aromatic surfaces, physical trapping in micro-/mesopores, and early microbial immobilization of nitrogen documented for biochar-manure systems and controlled-release nitrogen fertilizers with biochar addition (Firnass et al., 2023). (Hassan et al., 2024), (Lebrun et al., 2023). The delayed increase in $NO_3^-$ concentration inside the granule is consistent with the kinetics of nitrification regulated by oxygen and pH in porous carbon matrices, where ammonium retention and diffusion control the onset of nitrification activity. In the soil matrix, $NO_3^-$ exhibited an early pulse followed by attenuation, while intragranular $NO_3^-$ accumulated after day 70-signalling a switch from net consumption to net production once $O_2$ penetration and pH favoured nitrifiers (Yang et al., 2025; Zhang et al., 2024).

The temporal pattern of mineral N in soil and pellets-early ammonium release followed by progressive nitrate enrichment matches broader evidence on biochar-based nitrogen fertilizers (BBNFs). Because the incubation was conducted in a closed system without drainage, leaching, or plant uptake, mineral N could temporarily accumulate as $NH_4^+$-N before being converted to $NO_3^-$-N via nitrification. All treatments started from the same NH□□-N level, indicating homogeneous baseline conditions, and the elevated initial $NH_4^+$-N in the control likely reflects residual mineral N in cultivated topsoil from prior fertilisation and ongoing mineralisation of crop residues and native soil organic matter. The higher $NH_4^+$-N peaks in pellet-amended treatments are consistent with the substantial Kjeldahl-N pool introduced with the poultry-manure-based composites; under these conditions, only a fraction of the added N needs to appear transiently as $NH_4^+$ to generate the observed multi-fold differences before redistribution via nitrification, microbial immobilisation, and retention on exchange sites. Recent reviews conclude that BBNFs and biochar-coated fertilizers tend to slow N release, flatten peak mineral N concentrations and improve apparent N recovery (Banik et al., 2023), (Clough and Condron, 2010), (Yurong et al., 2022). The separation of intragranular and soil nitrate pools supports the concept that biochar-based formulations spatially compartmentalize N transformations. In a temperate arable field trial, Prommer et al. (2014) found that biochar decelerated organic N turnover but stimulated nitrification, leading to elevated nitrate in specific microenvironments rather than uniformly in the soil. Reviews of biochar and soil N dynamics emphasize that char particles provide microhabitats for nitrifiers, stabilizing nitrate temporarily and moderating its diffusion to the bulk solution (Clough et al., 2013). In line with these observations, pellets in our study behave as microreactors where ammonium is first retained and then nitrified, with part of the resulting nitrate remaining trapped within the granule matrix.

Nitrate retention in the pellets is also consistent with sorption studies. (Fidel et al., 2018) showed that both $NH_4^+$ and $NO_3^-$ sorption to biochars is largely electrostatic and strongly pH-dependent, with appreciable anion retention for chars rich in basic functional groups and minerals. (Hale et al., 2013) and (Gai et al., 2014) reported significant sorption of nitrate and ammonium by agricultural-residue biochars, with adsorption capacity governed by feedstock and pyrolysis temperature. Co-composting and ageing are known to enhance retention by promoting oxidation, mineral coatings, and pore development (Hagemann et al., 2017). The pronounced intragranular nitrate signal observed in our study suggests that manure-derived N, Ca/Mg inputs and porous biochar together create favourable conditions for both electrostatic and physical retention, as proposed for co-composted biochars and biochar-manure systems (Hagemann et al., 2017), (Kammann et al., 2015). Co-composting biochar with nutrient-rich organic substrates highlights the strong capacity of porous carbon granules to absorb and store nitrate. In work of Kammann et al., (2015) fresh wood biochar (BCpure) contained virtually no nitrate, whereas after six weeks of composting with cattle manure, straw, rock powder and soil, co-composted biochar (BCcomp) was heavily enriched in $NO_3^-$. Electro-ultrafiltration and sequential extraction revealed 2.0–2.2 g $NO_3^-$-N $kg^{-1}$ in readily desorbable fractions and 5.2 g $NO_3^-$-N $kg^{-1}$ in total, compared with 0.98 g $NO_3^-$-N $kg^{-1}$ in the compost. Thus, biochar granules stored over five times more nitrate per unit mass than the surrounding matrix, indicating that during incubation with manure, lime or gypsum, biochar-based pellets can progressively absorb nitrate via in-granule nitrification, diffusion-driven uptake and sorptive retention in organomineral coatings and pores. This temporal decoupling reduces the risk of external $NO_3^-$ spikes at the soil-pellet interface. Mineral co-additives modulated both mechanism and tempo. Gypsum likely contributed $Ca^{2+}$ bridging and flocculation, lowering colloid dispersion and P mobility (Ekholm et al., 2024). Lime strengthened the early buffering capacity of the soil, and a tendency toward greater acidification occurred in the later phase of incubation, which often occurs when alkaline additives are used together with the introduction of nitrogen susceptible to mineralization (Shi et al., 2024; Yang et al., 2025). Three design principles follow. (i) Temporal buffering: carbon-rich matrices that retain ammonium and delay nitrification synchronize N availability with crop demand, lowering early $NO_3^-$ peaks and potential leaching (Lebrun et al., 2023; Yang et al., 2025; Zhang et al., 2024). (ii) Chemical buffering: moderate ash alkalinity plus high CEC affords early pH stabilization without prolonged over liming (Hassan et al., 2024; Shi et al., 2024; Sriraj and Butnan, 2024). (iii) Hydro-ionic buffering: inclusion of gypsum (or low-rate lime) yields steady ECe patterns. (Ekholm et al., 2024). Operationally, pellet recipes that combine porous, moderately oxidized biochar; manure-derived organics; and gypsum (or modest lime) should minimize external $NO_3^-$ accumulation while maintaining availability. Because the amendments were applied as composite pellets, the responses observed in this incubation (pH dynamics, $NH_4^+$ retention, and N-release patterns) reflect the integrated action of biochar, manure and mineral additives, as well as pellet physical structure. The present design does not allow quantitative separation of component-specific contributions; such attribution would require single-component controls and/or a factorial mixture design. Importantly, the present study was intentionally designed to evaluate formulation-level performance, because in practice the pellets are applied as multi-component products rather than as individual constituents.

The study confirmed hypotheses, predicting that biochar-manure composites slow nitrogen release and enhance retention, was supported by the gradual ammonium decline and sustained total Kjeldahl nitrogen (>75% of initial N) in biochar-rich granules; assuming that gypsum moderates ionic strength and stabilizes ammonium while preventing excessive nitrate build-up, was validated by steady ECe increases (to 1100–1180 µS $cm^{-1}$) without salinity stress and delayed nitrate accumulation inside granules; proposing that lime elevates pH and steers nitrification under biochar buffering, was confirmed by early pH elevation to 6.7 followed by controlled acidification. Together, these findings demonstrate that compositional engineering of biochar-manure-mineral pellets achieved synchronized nitrogen transformation, pH stabilization, and balanced ionic release-fully supporting the experimental hypotheses.

## 5. Conclusions

The study showed that the composition of biochar-manure-mineral pellets controlled nitrogen transformation and soil stability. Gypsum and lime raised soil pH to 6.7 early in incubation, later moderating acidification, while mushroom substrate and fruit-stone biochar maintained pH >6.0 after 100 days. Electrical conductivity increased gradually to 1100–1180 µS $cm^{-1}$ in manure-gypsum variants, indicating steady ion release without salinity stress. Ammonium peaked at 250 mg N $kg^{-1}$ (G1–G3) and converted to nitrate exceeding 200 mg N $kg^{-1}$ by day 100. The addition of biochar to manure significantly enhanced ammonium retention by adsorbing $NH_4^+$ onto high-CEC carbon surfaces, thereby reducing its oxidation. Carbon-rich granules limited total Kjeldahl nitrogen loss to <25%, confirming strong N preservation. The system showed dual-phase kinetics-early nitrate rise in soil and delayed intragranular peaks-and three buffering effects: temporal (delayed nitrification), chemical (pH stabilization), and hydro-ionic (gradual ECe change), improving nitrogen-use efficiency and reducing leaching.

## Conflict of interest

The authors declare no conflict of interest. The authors declare that they have no known competing financial interests or personal relationships that could have influenced the work reported in this paper. This research did not involve human or animal subjects.

## Author Contributions

**Tomasz Niedziński** – Conceptualization, Data curation, Investigation, Methodology, Supervision, Visualization, Writing – original draft. **Wojciech Stępień** – Conceptualization, Funding acquisition, Methodology, Supervision, Validation, Writing – original draft. **Jan Łabętowicz** – Conceptualization, Supervision, Validation, Writing – review and editing). **Wiktoria Wierzchowska** – Investigation, Methodology, Visualization. **Bartłomiej Kowalczuk** – Investigation, Methodology, Visualization. **Katarzyna Szyszkowska** – Conceptualization, Data curation, Investigation, Methodology.

All authors read and approved the final manuscript.

## References

Abel, S., Peters, A., Trinks, S., Schonsky, H., Facklam, M., Wessolek, G., 2013. Impact of biochar and hydrochar addition on water retention and water repellency of sandy soil. Geoderma 202–203, 183–191. https://doi.org/10.1016/j.geoderma.2013.03.003

Alomari, L., Al-Issa, T., Kiyyam, M.A., Al Tawaha, A.R., 2024. The Impact of Biochar and Compost as Soil Amendments, Combined with Poultry Manure, on the Growth, Yield, and Chemical Composition of Lettuce (Lactuca sativa). Journal of Ecological Engineering 25, 12–28. https://doi.org/10.12911/22998993/186723

Atkinson, C.J., Fitzgerald, J.D., Hipps, N.A., 2010. Potential mechanisms for achieving agricultural benefits from biochar application to temperate soils: A review [Review]. Plant and Soil 337(1), 1–18. https://doi.org/10.1007/s11104-010-0464-5

Banik, C., Bakshi, S., Laird, D., Smith, R., Brown, R., 2023. Impact of biochar-based slow-release N-fertilizers on maize growth and nitrogen recovery efficiency. Journal of Environmental Quality 52. https://doi.org/10.1002/jeq2.20468

Calvano, C., Tamborrino, A., 2022. Valorization of Olive By-Products: Innovative Strategies for Their Production, Treatment and Characterization. Foods 11, 768. https://doi.org/10.3390/foods11060768

Chintalaa, R., Mollinedo, J., Schumacher, T., Malo, D., Julson, J., 2013. Effect of biochar on chemical properties of acidic soil (vol 60, pg 393, 2012). Archives of Agronomy and Soil Science 61, 889–889. https://doi.org/10.1080/03650340.2014.1002189

Clough, T., Condron, L.M., 2010. Biochar and the Nitrogen Cycle: Introduction. Journal of environmental quality 39, 1218–1223. https://doi.org/10.2134/jeq2010.0204

Clough, T., Condron, L.M., Kammann, C., Müller, C., 2013. A Review of Biochar and Soil Nitrogen Dynamics. Agronomy 3, 275–293. https://doi.org/10.3390/agronomy3020275

Ekholm, P., Ollikainen, M., Punttila, E., Ala-Harja, V., Riihimäki, J., Kiirikki, M., Begum, K., 2024. Gypsum Amendment of Agricultural Fields Decreases Phosphorus Losses – Evidence on a Catchment Scale. https://doi.org/10.2139/ssrn.4694131

Ekholm, P., Valkama, P., Röman, E., Kiirikki, M., Lahti, K., Pietola, L., 2012. Gypsum amendment of soils reduces phosphorus losses in an agricultural catchment. Agricultural and Food Science 21, 279–291. https://doi.org/10.23986/afsci.6831

Fauzan, M., Arafat, S., Irawan, A., 2025. Enhancing saline soil fertility through biochar and organic manure combinations: An incubation study. Journal of Ecological Engineering 26, 82–95. https://doi.org/10.12911/22998993/204560

Fidel, R., Laird, D., Spokas, K., 2018. Sorption of ammonium and nitrate to biochars is electrostatic and pH-dependent. Scientific Reports 8. https://doi.org/10.1038/s41598-018-35534-w

Firnass, M., Pandian, K., Kuppusamy, S., Krishnaveni, D., 2023. Synthesis of biochar-embedded slow-release nitrogen fertilizers; Mesocosm and field scale evaluation for nitrogen use efficiency, growth and rice yield. Soil Use and Management 40. https://doi.org/10.1111/sum.12959

Fornes, F., Lidón, A., Belda, R.M., Macan, G.P.F., Cayuela, M.L., Sánchez-García, M., Sánchez-Monedero, M.A., 2024. Soil fertility and plant nutrition in an organic olive orchard after 5 years of amendment with compost, biochar or their blend. Scientific Reports 14(1), 16606. https://doi.org/10.1038/s41598-024-67565-x

Fávero, C., Leal, C., Churka Blum, S., Barth, G., José, G., 2006. Surface application of lime ameliorates subsoil acidity and improves root growth and yield of wheat in an acid soil under no-till system. Scientia Agricola 63. https://doi.org/10.1590/S0103-90162006000500013

Gai, X., Wang, H., Liu, J., Zhai, L., Liu, S., Ren, T., Liu, H., 2014. Effects of Feedstock and Pyrolysis Temperature on Biochar Adsorption of Ammonium and Nitrate. PloS one 9, e113888. https://doi.org/10.1371/journal.pone.0113888

Glaser, B., Lehmann, J., Zech, W., 2002. Ameliorating Physical and Chemical Properties of Highly Weathered Soils in the Tropics with Charcoal – a Review. Biology and Fertility of Soils 35. https://doi.org/10.1007/s00374-002-0466-4

Goulding, K., 2016. Soil acidification and the importance of liming agricultural soils with particular reference to the United Kingdom. Soil Use and Management 32. https://doi.org/10.1111/sum.12270

Hagemann, N., Kammann, C., Schmidt, H.P., Kappler, A., Behrens, S., 2017. Nitrate capture and slow release in biochar amended compost and soil. Plose One 12, e0171214. https://doi.org/10.1371/journal.pone.0171214

Hale, S., Alling, V., Martinsen, V., Mulder, J., Breedveld, G., and Cornelissen, G., 2013. The sorption and desorption of phosphate-P, ammonium-N and nitrate-N in cacao shell and corn cob biochars. Chemosphere 91. https://doi.org/10.1016/j.chemosphere.2012.12.057

Hassan, M., Huang, G., Munir, R., Khan, T., Noor, M., 2024. Biochar Co-Compost: A Promising Soil Amendment to Restrain Greenhouse Gases and Improve Rice Productivity and Soil Fertility. Agronomy 14, 1583. https://doi.org/10.3390/agronomy14071583

Hou, T., Chen, N., Tong, S., Li, B., He, Q., Feng, C., 2018. Enhancement of rice bran as carbon and microbial sources on the nitrate removal from groundwater. Biochemical Engineering Journal 148. https://doi.org/10.1016/j.bej.2018.07.010

Igalavithana, A., Lee, S.E., Lee, Y., Tsang, D., Rinklebe, J., Ok, Y.S., 2017. Heavy metal immobilization and microbial community abundance by vegetable waste and pine cone biochar of agricultural soils. Chemosphere 174. https://doi.org/10.1016/j.chemosphere.2017.01.148

ISO 10390: 2005. Soil Quality – Determination of pH. In.

ISO 11261:1995. Determination of Total Nitrogen – Modified Kjeldahl Method. In.

IUSS Working Group WRB., 2015. International soil classification system for naming soils and creating legends for soil maps, World Soil Resources Reports 106. Rome: FAO.

Jeffery, S., Verheijen, F.G.A., van der Velde, M., Bastos, A.C., 2011. A quantitative review of the effects of biochar application to soils on crop productivity using meta-analysis. Agriculture, Ecosystems and Environment 144(1), 175–187. https://doi.org/10.1016/j.agee.2011.08.015

Kammann, C., Schmidt, H.P., Messerschmidt, N., Linsel, S., Müller, C., Koyro, H.W., Joseph, S., 2015. Erratum: Plant growth improvement mediated by nitrate capture in co-composted biochar. Scientific Reports 5, 11080;. https://doi.org/10.1038/srep11080

Lebrun, M., Zahid, Z., Bednik-Dudek, M., Medyńska-Juraszek, A., Száková, J., Brtnický, M., Trakal, L., 2023. Combined biochar and manure addition to an agricultural soil benefits fertility, microbial activity, and mitigates manure-induced CO2 emissions. Soil Use and Management 40. https://doi.org/10.1111/sum.12997

Lehmann, J., Rillig, M., Thies, J., Masiello, C., Hockaday, W., Crowley, D., 2011. Biochar effects on soil biota – A review. Soil Biology and Biochemistry 43, 1812–1836. https://doi.org/10.1016/j.soilbio.2011.04.022

Liang, B., Lehmann, J., Solomon, D., Kinyangi, J., Grossman, J., O'Neill, B., Neves, E.G., 2006. Black carbon increases cation exchange capacity in soils. Soil Science Society of America Journal 70(5), 1719–1730. https://doi.org/10.2136/sssaj2005.0383

Malinska, K., Zabochnicka, M., and Dach, J., 2014. Effects of biochar amendment on ammonia emission during composting of sewage sludge. Ecological Engineering 71, 474–478. https://doi.org/10.1016/j.ecoleng.2014.07.012

Mandal, S., Thangarajan, R., Bolan, N., Sarkar, B., Khan, N., Ok, Y.S., Naidu, R., 2015. Biochar-induced concomitant decrease in ammonia volatilization and increase in nitrogen use efficiency by wheat. Chemosphere 142. https://doi.org/10.1016/j.chemosphere.2015.04.086

Niedziński, T., Rutkowska, B., Łabętowicz, J., Szulc, W., 2023. Effect of Deep Placement Fertilization on the Distribution of Biomass, Nutrients, and Root System Development in Potato Plants. Plants 12(9), 1880. https://doi.org/10.3390/plants12091880

Niedziński, T., Sierra, M.J., Łabętowicz, J., Noras, K., Cabrales, C., Millán, R., 2021. Release of nitrogen from granulate mineral and organic fertilizers and its effect on selected chemical parameters of soil. Agronomy 11(10), 1981. https://doi.org/10.3390/agronomy11101981

Niedziński, T., Łabętowicz, J., Stępień, W., Pęczek, T., 2023. Analysis of the Use of Biochar from Organic Waste Pyrolysis in Agriculture and Environmental Protection. Journal of Ecological Engineering 24(4), 85–98. https://doi.org/10.12911/22998993/159347

Oarga, A., Jenssen, P., and Griessler Bulc, T., 2019. A comparison of various bulking materials as a supporting matrix in composting blackwater solids from vacuum toilets. Journal of Environmental Management 243, 78–87. https://doi.org/10.1016/j.jenvman.2019.05.005

Oarga, A., Mihelic, R., Walochnik, J., Griessler Bulc, T., 2016. Composting of the solid fraction of blackwater from a separation system with vacuum toilets – Effects on the process and quality. Journal of Cleaner Production 112. https://doi.org/10.1016/j.jclepro.2015.07.080

Olifir, Y., Habryiel, A., Partyka, T., Havryshko, O., Konyk, H., Panakhyd, H., Ivaniuk, V., 2024. The dynamics of mobile iron compounds and redox potential of Albic Pantostagnic Luvisol depending on long-term various fertilisation. Soil Science Annual 75, 1–10. https://doi.org/10.37501/soilsa/195939

Pandian, K., Vijayakumar, S., Firnass, M., Subramanian, P.C.S., 2024. Biochar – a sustainable soil conditioner for improving soil health, crop production and environment under changing climate: a review. Frontiers in Soil Science 4, 1376159. https://doi.org/10.3389/fsoil.2024.1376159

Prommer, J., Wanek, W., Hofhansl, F., Trojan, D., Offre, P., Urich, T., Hood--Nowotny, R., 2014. Biochar Decelerates Soil Organic Nitrogen Cycling but Stimulates Soil Nitrification in a Temperate Arable Field Trial. PloS One 9, e86388. https://doi.org/10.1371/journal.pone.0086388

Quilliam, R., Marsden, K., Gertler, C., Rousk, J., DeLuca, T., Jones, D., 2012. Nutrient dynamics, microbial growth and weed emergence in biochar amended soil are influenced by time since application and reapplication rate. Agriculture Ecosystems and Environment 158, 192–199. https://doi.org/10.1016/j.agee.2012.06.011

Rebecca, E., 2023. Liming remediates soil acidity and improves crop yield and profitability – a meta-analysis. Frontiers in Agronomy 5. https://doi.org/10.3389/fagro.2023.1194896

Regulation (EU) 2019/1009 of the European Parliament and of the Council of 5 June 2019 laying down rules on the making vailable on the market of EU fertilising products and amending Regulations (EC) No 1069/2009 and (EC) No 1107/2009 and repealing Regulation (EC) No 2003/2003.

Shi, G., Hou, R., Li, T., Fu, Q., Chen, Q., Xue, P., Yang, X., 2024. Effects of biochar on the transformation and utilization of nitrogen fertilizer in the black soil region of Northeast China. Science of The Total Environment 953, 176218. https://doi.org/10.1016/j.scitotenv.2024.176218

Siewruk, K., Szulc, W., 2023. Assessment of the effect of intensive agricultural production on nutrient movement in soil. Soil Science Annual 74, 1–7. https://doi.org/10.37501/soilsa/171629

Skuta, I., Kołodziej, B., Filipek-Mazur, B., Antonkiewicz, J., 2025. The Use of Carbonate-Clay Flour, Sewage Sludge and Waste Sulfate Sulfur as Fertilizer Agents. Resources 14(7), 113. https://doi.org/10.3390/resources14070113

Sriraj, P., Butnan, S., 2024. Lasting effects of the co-application of rice husk biochar with cattle manure and compost on soil and corn. Soil Science Annual 75(4), Article 195816. https://doi.org/10.37501/soilsa/195816

Sumner, M.E., Shahandeh, H., Bouton, J., and Hammel, J., 1986. Amelioration of an acid soil profile through deep liming and surface application of gypsum. Soil Science Society of America Journal 50(5), 1254–1258. https://doi.org/10.2136/sssaj1986.03615995005000050034x

Sun, X., Yang, X., Hu, Z., Liu, F., Zijian, X., Li, S., Bol, R., 2024. Biochar effects on soil nitrogen retention, leaching and yield of perennial citron daylily under three irrigation regimes. Agricultural Water Management 296, 108788. https://doi.org/10.1016/j.agwat.2024.108788

Wang, C., Luo, D., Zhang, X., Huang, R., Cao, Y., Liu, G., Wang, H., 2022. Biochar-based slow-release of fertilizers for sustainable agriculture: A mini review. Environmental Science and Ecotechnology 10, 100167. https://doi.org/10.1016/j.ese.2022.100167

Yang, W., Zhang, L., Wang, Z., Zhang, J., Li, P., Su, L., 2025. Effects of biochar and nitrogen fertilizer on microbial communities, $CO_2$ emissions, and organic carbon content in soil. Scientific Reports 15. https://doi.org/10.1038/s41598-025-94784-7

Yurong, G., Fang, Z., Van Zwieten, L., Bolan, N., Dong, D., Quin, B., Chen, W., 2022. A critical review of biochar-based nitrogen fertilizers and their effects on crop production and the environment. Biochar 4. https://doi.org/10.1007/s42773-022-00160-3

Zhang, M., Xie, W., Zhong, X., Wang, Y., Li, S., Zhou, Y., Wang, C., 2024. The impact of combined application of biochar and fertilizer on the biochemical properties of soil in soybean fields. PeerJ 12, e18172. https://doi.org/10.7717/peerj.18172

## Uwalnianie azotu i zmiana właściwości gleby przez granulaty wytworzone z biowęgla, obornika z dodatkiem składników mineralnych

**Słowa kluczowe**

Granulaty z biowęgla i obornika
Przemiana azotu
Nawozy o kontrolowanym uwalnianiu
Zdolność buforowania gleby
Zrównoważone zarządzanie składnikami odżywczymi

**Streszczenie**

Granulaty wytworzone z biowęgla, obornika i dodatków mineralnych inkubowano w glebie przez 100-dni przeprowadzone w kontrolowanych warunkach laboratoryjnych, w celu wyjaśnienia dynamiki uwalniania azotu oraz buforujących właściwości chemicznych gleby. W glebie płowej (Luvisol) inkubowano osiem różnych granulatów wytworzonych z biowęgli, obornika drobiowego, gipsu, wapna oraz dodatków organicznych, zaprojektowanych tak, aby reprezentowały odmienne właściwości chemiczne. Wykazano iż, inkubacja granulatów zawierających wapno bądź gips wywołała wzrost pH gleby do 6,7, następnie wystąpił spadek wartości pH gleby, dla granulatów zawierających podłoże popieczarkowe i biowęgiel z pestek owoców wykazano niemal neutralną reakcję gleby (pH >6,0) pod koniec inkubacji. Inkubacja granulatów zawierających obornik i gips spowodowała przyrost przewodności elektrycznej z 102 do 1100–1180 µS $cm^{-1}$ przez stopniowe uwalnianie jonów, bez ryzyka wystąpienia stresu solnego. Dla granulatów G1-G3 zmierzono stężenie jonu amonowego w glebie wynoszące blisko 250 mg N kg–1 (G1-G3), który następnie przekształcił się w formę azotanową, osiągając stężenie powyżej 200 mg N $kg^{-1}$ w dniu 100 inkubacji. Tempo uwolnienia azotu Kjeldahla z granulatów było umiarkowane, na koniec inkubacji wykazano 62–92% początkowej zawartości. Uzyskane wyniki ujawniają dwufazową kinetykę przemian związków azotu: akumulację azotanów w glebie, a następnie przyrost stężenia azotanów wewnątrz granulatów, spowodowane dyfuzją tlenu i nitryfikacją zależną od pH. Połączenie biowęgla, gipsu i wapna umożliwia uzyskanie trzech synergicznych efektów buforujące: czasowego (opóźniona nitryfikacja), chemicznego (stabilizacja pH) i hydrojonowego (stopniowa ewolucja ECe). Wyniki te stanowią podstawę do projektowania granulatów nawozowych organiczno-mineralnych, które umożliwiają synchronizację uwalniania azotu z aktywnością mikroorganizmów glebowych jednocześnie minimalizując zakwaszenie i straty składników odżywczych.